

1 **Drainage rearrangements and in situ diversification of an endemic freshwater fish**
2 **genus from northeastern Brazilian rivers**

3
4 **Running title:** Phylogeography of *Nematocharax*

5
6 Silvia Britto Barreto^a, L. Lacey Knowles^b, Rilquer Mascarenhas^a, Paulo Roberto Antunes de
7 Mello Affonso^c, and Henrique Batalha-Filho^a

8
9 ^aNational Institute of Science and Technology in Interdisciplinary and Transdisciplinary
10 Studies in Ecology and Evolution (INCT IN-TREE), Institute of Biology, Federal University
11 of Bahia, 147 Barão de Jeremoabo St., 40170-115, Salvador – BA, Brazil

12
13 ^bDepartment of Ecology and Evolutionary Biology, Museum of Zoology, University of
14 Michigan, 1105 N University Ave., 48109, Ann Arbor – MI, USA

15
16 ^cDepartment of Biological Sciences, State University of Southwestern Bahia, José Moreira
17 Sobrinho Ave., 45208-091, Jequié – BA, Brazil

18
19 **Corresponding author:** Silvia Britto Barreto (<https://orcid.org/0000-0001-8780-1959>)
20 Address: Institute of Biology, Federal University of Bahia, 147 Barão de Jeremoabo St.,
21 40170-115, Salvador – BA, Brazil; Telephone: +55 71 3283 6556; Fax: +55 71 3283 6511;
22 E-mail address: sbrittob@gmail.com

23
24
25
26
27
28
29
30
31
32

This is the author manuscript accepted for publication and has undergone full peer review but has not been through the copyediting, typesetting, pagination and proofreading process, which may lead to differences between this version and the [Version of Record](#). Please cite this article as [doi: 10.1111/fwb.13879](https://doi.org/10.1111/fwb.13879)

This article is protected by copyright. All rights reserved

33

34

35 **ABSTRACT**

36

37 1. Drainage rearrangements, either headwater captures or coastal paleodrainages formed
38 when sea level was low, are often invoked to explain connectivity and isolation among fish
39 populations. Unraveling these events is crucial for understanding the evolutionary processes
40 that have shaped the genetic diversity and differentiation in freshwater fishes, which is
41 especially relevant in regions with high endemism and species richness.

42 2. Here, we analyze mitochondrial (COI) and genomic (RADseq) data to test the putative
43 effects of the current configuration of basins and historical drainage rearrangements on the
44 genetic structuring of a characid fish (*Nematocharax*) endemic to a largely overlooked
45 Neotropical freshwater ecoregion – the Northeastern Mata Atlantica (NMA). Bathymetric
46 and geomorphological data were also used to generate hypotheses for two potential routes of
47 dispersal (headwater captures and coastal paleodrainages).

48 3. We found that the divergence between lineages from the highlands of the Brazilian shield
49 and the lowlands occurred during the Mio-Pliocene (i.e., divergence between *N. varii* and *N.*
50 *venustus*), followed by divergence events within *N. venustus* in lowland basins during the
51 Pleistocene. The general distribution of genetic variation in *N. venustus* seems to reflect the
52 current configuration of basins, suggesting long-term isolation, but a subset of the inferred
53 drainage rearrangements have facilitated movement among these watersheds, which is
54 supported by both mtDNA and genomic data.

55 4. Our results suggest that the NMA river basins have had their own independent histories,
56 except for some past temporary connections that allowed dispersal events and multiple
57 independent colonization of basins, as seen in the Contas and Cachoeira river systems.

58 5. Estimating when and where connections between river basins may have occurred is
59 fundamental to understand the role of different historical processes structuring divergence in
60 freshwater fish species.

61

62 **Keywords:** coastal basins; genetic structure; headwater captures; Neotropical fish;
63 paleodrainages.

64

65 **INTRODUCTION**

66

67 River networks represent complex systems whose architecture may vary greatly over
68 both space and time, affecting the evolution and distribution of freshwater organisms
69 (Hughes et al., 2009; Dias et al., 2014). Drainage rearrangements, in particular headwater
70 captures and coastal paleodrainages, are considered potential drivers of diversification or
71 divergence within species by providing periodic connections between previously isolated
72 rivers such that species can expand their ranges into river segments (e.g. Thomaz et al., 2015;
73 Lima et al., 2017; Shelley et al., 2020). Unlike terrestrial and marine species, obligate
74 freshwater fishes depend on stream connectivity to move among river basins and colonize
75 new drainages. Therefore, isolation among populations and species lineages may be
76 pronounced in scenarios with limited dispersal opportunities, resulting in long-term isolation
77 (Carvajal-Quintero et al., 2019). On the other hand, some fish may show shared haplotypes
78 among drainages in cases where past episodic connections allowed genetic exchange between
79 adjacent basins (Thomaz & Knowles, 2018).

80 The complex evolutionary history of the Neotropical ichthyofauna is still not fully
81 understood, given its high species richness and the variable topography of the hydrographic
82 systems in this region (Albert & Reis, 2011). Not only does the current configuration of
83 disconnected basins represent barriers to gene flow and contribute to divergence processes by
84 allopatry, but recent studies have also shown the effects of past geomorphological events on
85 population genetic diversity and differentiation in Neotropical fishes (e.g. Thomaz et al.,
86 2017; Camelier et al., 2018; Lima et al., 2021). Among these events, past connections
87 between today's isolated basins are forged by either headwater captures or coastal
88 paleodrainages, which can facilitate dispersal between drainages and range expansion, and
89 possibly promote speciation. Headwater capture involves the splitting and merging of
90 drainages through processes influenced by the steepness, amount of rainfall, and type
91 (hardness) of the underlying rock (Bishop, 1995; Albert et al., 2018). Coastal paleodrainages
92 also provided past connections among river basins due to sea level retreats associated with
93 glacial cycles that largely exposed the continental shelf, which occurred mainly during the
94 Pleistocene (Weitzman et al., 1988). This type of paleo-connection is especially relevant in
95 small to mid-size coastal basins, in which the near-shore marine environment can function as
96 a barrier for strictly freshwater fishes. In large river systems, such as the Amazon and
97 Orinoco rivers along the northern coast of South America, the spreading of freshwater plumes
98 is hypothesized to facilitate dispersal of freshwater fishes among coastal basins regardless of
99 potential Pleistocene river extensions (Winemiller & Willis, 2011).

100 Valuable information on the occurrence of drainage rearrangements can be provided
101 by genetic data, for instance by revealing the presence of closely related groups in adjacent
102 basins or secondary contact between populations that were previously geographically isolated
103 in different basins (BurrIDGE et al., 2006; Schwarzer et al., 2012). However, bathymetric and
104 geomorphological evidence are crucial complementary data that can be used to generate
105 hypotheses of past connections between river systems (e.g. Thomaz & Knowles, 2020).
106 Furthermore, the predominance of headwater captures and coastal paleodrainages in
107 structuring fish communities is expected to vary regionally. For example, the width of the
108 continental shelf differs along the Brazilian coast; the northeast region is considerably
109 narrower compared to the southeast (Martins & Coutinho, 1981). Consequently, connections
110 via coastal paleodrainages are less likely in the northeast (above the Abrolhos Bank) during
111 periods of marine regression (Thomaz & Knowles, 2018). On the other hand, headwater
112 captures may have provided several connections in northeastern Brazil (Ribeiro, 2006).

113 With limited information on the biogeographic history of freshwater organisms from
114 northeastern Brazilian coastal basins like those of the Northeastern Mata Atlantica (NMA)
115 ecoregion (Abell et al., 2008), it is not clear the extent to which historical events have shaped
116 the evolution of the ichthyofauna. This is especially the case in fish communities that are
117 poorly understood despite high levels of endemism, such as the NMA ecoregion, which
118 includes coastal lowlands and adjacent highlands from the Espinhaço Range, and where up to
119 61% of species are endemic (Albert et al., 2011). Parallel and isolated river basins of the
120 NMA, which is bordered by the São Francisco River in the north and west, and the Paraíba
121 do Sul River in the south (Hales & Petry, 2015), have no doubt triggered high levels of
122 endemism. The NMA ecoregion is subdivided into three biogeographic regions (Northern,
123 Central, and Southern), with different species compositions and independent histories
124 (Camelier & Zanata, 2014). However, within each region, and especially in the Central
125 region, faunal distributions suggest past connections between presently isolated river basins
126 (i.e., the Contas, Almada, Cachoeira, Una, Pardo, and Jequitinhonha river basins; Figure 1).

127 One taxon that supports the hypothesis of some shared history among the Central
128 NMA basins is the endemic fish *Nematocharax venustus* (Camelier & Zanata, 2014), a small
129 member (up to 60 mm in standard length) of the Characidae family. The species was once
130 considered vulnerable to extinction due to impacts on its habitats such as removal of riparian
131 vegetation and introduction of exotic species (Menezes & Lima, 2008). Outstanding features
132 of *N. venustus* include sexual dimorphism and morphological and genetic variation among its
133 populations (Menezes et al., 2015; Barreto, Cioffi, et al., 2016; Barreto, Nunes, et al., 2016).

134 On the other hand, its only congener, *N. varii*, is known for only two nearby localities in a
135 tributary of the Upper Contas River situated around 530 m elevation on the Chapada
136 Diamantina highlands (Barreto et al., 2018). In this sense, reconstructing the evolutionary
137 history of *Nematocharax* populations can help disentangle the role of drainage
138 rearrangements on the evolution of freshwater fishes.

139 Here we used cytochrome c oxidase subunit I (COI) sequences and restriction site-
140 associated DNA (RADseq) markers to investigate the spatial and temporal patterns of
141 population divergence across the entire range of *Nematocharax* (including both *N. venustus*
142 and *N. varii*). Specifically, by considering the genetic data jointly with bathymetric,
143 geological, and geomorphological information, we tested the putative effects of the current
144 configuration of basins and historical drainage rearrangements, either headwater captures or
145 coastal paleodrainages, on the phylogeographic structuring of *Nematocharax*. We hope that
146 by combining these different data sources to unravel the population history of this endemic
147 fish genus we can shed light on the biogeographic history of the NMA region's aquatic biota.

148

149 **METHODS**

150

151 **Sampling**

152

153 Tissue samples from 182 specimens of *Nematocharax*, including *N. venustus* and *N.*
154 *varii*, were obtained from 37 collection sites across the entire distribution of the genus (i.e.,
155 the Contas, Almada, Cachoeira (including the Santana River), Una, Pardo, and Jequitinhonha
156 river basins; Figure 1). The collection license (number 51856-2) was provided by the Instituto
157 Chico Mendes de Conservação da Biodiversidade (ICMBio/SISBIO), and the ethical
158 approval for this study was obtained from the Ethics Committee of Utilization of Animals
159 from the Universidade Estadual do Sudoeste da Bahia (CEUA/UESB, number 71/2014). All
160 collected fish are deposited in the ichthyological collection of the Universidade Federal da
161 Bahia (UFBA) (see Table S1 for details).

162

163 **Sanger sequencing**

164

165 We investigated the genetic structure of *Nematocharax* at a broad spatial scale using
166 COI sequences for all samples. Total DNA was extracted from ethanol preserved tissues
167 (muscle or fin) using the Wizard Genomic DNA Purification kit (Promega, Madison, USA).

168 Six hundred and fifty base pairs (bp) of COI were amplified with the primers FishF2_t1 and
169 FishR2_t1 (Ward et al., 2005) following the same conditions and steps described in Barreto,
170 Nunes, et al. (2016). Sequencing in both directions was performed at the Gonçalo Moniz
171 Research Center (FIOCRUZ-Bahia) using the BigDyeTerminator v3.1 Cycle Sequencing
172 Ready Reaction kit (Applied Biosystems, Foster City, USA).

173 Forward and reverse electropherograms were assembled into contigs using the
174 program CodonCode Aligner version 6.0 (CodonCode Corporation;
175 <http://www.codoncode.com/aligner/>). Sequences were then aligned with the ClustalW
176 Multiple Alignment tool (Thompson et al., 1994) in BioEdit 7.1.9 and deposited in GenBank
177 (accession numbers MN011168-MN011188 and MN011203-MN011363). In addition to the
178 182 sequences generated specifically for this study, other 113 COI sequences of
179 *Nematocharax* (including five additional localities) were downloaded from GenBank and
180 BOLD (Barcode of Life Data Systems; <http://www.boldsystems.org/>) (acc. num. PIABA001-
181 14 to PIABA091-14, MG025937 to MG025944, and MN011189-MN011202 from Barreto,
182 Nunes, et al., 2016, Barreto et al., 2018, and Barreto et al., 2020, respectively; see Table S1
183 for further details), totaling 295 samples for the COI dataset (274 for *N. venustus* and 21 for
184 *N. varii*).

185

186 **Analyses of mitochondrial DNA**

187

188 A time-calibrated phylogeny was estimated in BEAST 1.8.4 (Drummond et al., 2012)
189 to assess the timing of lineage diversification and test whether it is consistent with the
190 Pleistocene, during which glacial cycles reduced the sea level by up to 130 m below the
191 current level in the Last Glacial Maximum (LGM) (Clark et al., 2009). In addition to the
192 sequences of *Nematocharax*, we included as outgroups sequences representing three genera
193 closely related to it (Oliveira et al., 2011), which are: *Hasemanina nana* (acc. num.
194 NC_022724), *Hemigrammus marginatus* (acc. num. HM906014), and *Moenkhausia costae*
195 (acc. num. HM405163). The HKY+I+G substitution model was selected in jModelTest 2
196 (Darriba et al., 2012) according to the Akaike Information Criterion (AIC). We used a
197 substitution rate for fish mtDNA (1% per Myr; e.g. Thomaz et al., 2015) under a strict clock
198 model and speciation Yule process as a tree prior to perform the analysis, considering the
199 presence of different species in the dataset and highly differentiated mtDNA lineages within
200 *Nematocharax*, some of them already known from Barreto, Nunes et al. (2016) and Barreto et
201 al. (2018). Two independent Markov Chain Monte Carlo (MCMC) runs were carried out,

202 each consisting of 100 million generations, sampling every 1,000 generations, with the first
203 10% of the runs excluded as burn-in. Convergence was checked using Tracer 1.7.1 (Rambaut
204 et al., 2018), which we also used to ensure that all Effective Sample Size (ESS) values were
205 >200. Independent runs were combined in LogCombiner 1.8.4, and the Maximum Clade
206 Credibility (MCC) tree was generated in TreeAnnotator 1.8.4 and then visualized in FigTree
207 1.4.3 (<http://tree.bio.ed.ac.uk/software/figtree/>).

208 We performed a Bayesian analysis of genetic differentiation among samples of *N.*
209 *venustus* using the software BAPS 6.0 (Bayesian Analysis of Population Structure; Corander
210 & Marttinen, 2006); *N. varii* was not included in the analysis due to insufficient geographic
211 sampling. We conducted a population mixture analysis based on a “clustering with linked
212 loci” setting the maximum number of clusters (*K*) to 15. In addition, for each mitochondrial
213 lineage, we calculated the nucleotide diversity (π) and number of haplotypes in DnaSP 6
214 (Rozas et al., 2017) and evaluated putative signs of demographic expansion using Tajima’s *D*
215 (Tajima, 1989) and Fu’s *F_s* (Fu, 1997), with default settings. The significance of the tests was
216 obtained from 1,000 coalescent simulations.

217

218 **Genomic data generation and assembly**

219

220 Genomic data for a subset of 23 representative individuals of the 10 mtDNA lineages
221 (see Results) were generated using RADseq. Specifically, the ezRAD libraries (one per
222 sample) were prepared according to Toonen et al. (2013) and Knapp et al. (2016) from total
223 DNA extracted from muscle tissues using the DNeasy Blood & Tissue kit (Qiagen, Hilden,
224 Germany). Briefly, the DNA was digested with the *DpnII* restriction endonuclease (New
225 England Biolabs, Ipswich, USA) and purified by adding a 1.8X volume of AMPure XP
226 magnetic beads (Beckman Coulter, Brea, USA), which were also used to size select 150-350
227 bp DNA fragments. A-tailing, adapter ligation, enrichment by PCR, and additional clean-up
228 steps were performed using the TruSeq Nano DNA HT Library Prep kit (Illumina, San
229 Diego, USA). All libraries were quantified on a Qubit 2.0 Fluorometer using the Qubit
230 dsDNA BR Assay kit (Thermo Fisher Scientific, Waltham, USA) and an Agilent Bioanalyzer
231 2100 using DNA 1000 chips (Agilent Technologies, Santa Clara, USA). Paired-end
232 sequencing (2x75 bp) was performed on an Illumina NextSeq 500 sequencer at the Genome
233 Investigation and Analysis Laboratory (GENIAL) core facility (CEFAP-USP, São Paulo,
234 Brazil), using a Mid-Output v2 kit with 150 cycles.

235 After sequencing, the raw reads of each individual were demultiplexed using bcl2fastq
236 1.8.4 (Illumina; <http://support.illumina.com/downloads.html>) and processed with ipyrad
237 version 0.7.28 (Eaton, 2014; <http://ipyrad.readthedocs.io/>). Filtered reads were assembled *de*
238 *novo* with a clustering threshold of 0.85 and a minimum read depth of 6X, with the most
239 stringent filtering to remove Illumina adapters, and 15 bp trimmed from the 3' ends to reduce
240 error rates due to low quality of reads (Del Fabbro et al., 2013) (see Table S2 for more details
241 on the parameters used in ipyrad). The RADseq data resulted in a total of 19,099 filtered loci
242 and 61,696 SNPs, excluding loci with >50% missing data. The number of filtered reads per
243 sample varied from 1,609,668 to 6,021,549 (Table S3). Individuals from the Jequitinhonha
244 River basin were poorly sequenced and therefore were not included in the genomic analyses.

245

246 **Analyses of RADSeq data**

247

248 For the genomic data, we estimated phylogenetic relationships using the concatenated
249 dataset, as well as using the multispecies coalescent (MSC) model to accommodate different
250 genealogical histories among loci due to phenomena such as incomplete lineage sorting (ILS;
251 Rannala et al., 2020). The concatenated data were used to conduct a Maximum Likelihood
252 (ML) analysis under a GTRAC model in RAxML 8.2.10 (Stamatakis, 2014) and a Bayesian
253 analysis in MrBayes 3.2.6 (Ronquist et al., 2012), both through the CIPRES Science Gateway
254 Portal (Miller et al., 2010). For the Bayesian inference, the best model of nucleotide evolution
255 was inferred as GTR+I+G with jModelTest 2. We performed four million generations using
256 two runs of four chains each sampled every 500 generations, with a 10% burn-in. On the
257 other hand, the MSC analysis was conducted in SVDquartets (Chifman & Kubatko, 2014)
258 implemented in PAUP* 4.0 (Swofford, 2003) using a single SNP per locus.

259 The analysis of population structure within *N. venustus* was conducted using the
260 sparse non-negative matrix factorization (sNMF) algorithm (Frichot et al., 2014). We tested
261 *K*-values (number of ancestral populations) ranging from 1 to 15, running 200 replicates for
262 each *K* under four different alpha regularization parameter values (i.e., 1, 10, 100, and 1000)
263 to test the robustness of the results. The cross-entropy criterion was used to select the best *K*-
264 value.

265 To test which historical demographic scenario is more likely to have occurred with the
266 lineages of *Nematocharax*, we used the coalescent-based program fastsimcoal2 (Excoffier et
267 al., 2013) in order to compare divergence models with and without gene flow. Despite the
268 difficulties in identifying genetic signatures of drainage rearrangement events (Souza et al.,

269 2020), these models can provide insights into the effects of gene flow on populations,
270 allowing to test whether the lineages have been isolated for long periods of time or historical
271 gene flow has occurred among currently isolated river basins, which may indicate that
272 drainage rearrangements provided effective connections between watersheds.

273 Because fastsimcoal2 requires no missing data, the tests were conducted in separate
274 analyses of four datasets containing different subsets of individuals (Table S4). Specifically,
275 pairwise divergences were estimated for each of the four divergences based on the
276 relationships from the MSC tree estimated with SVDquartets. Distinct assemblies were made
277 in ipyrad for each of the four datasets (i.e., for individuals from the: i-ii, iii-iv, v-vi, and vii-
278 viii lineages; see Results) retaining only loci without missing data (details on the ipyrad
279 parameters are reported in Table S2). The joint Site Frequency Spectrum (SFS) was obtained
280 using the Python script ‘easySFS.py’ (<http://github.com/isaacovercast/easySFS>) for each
281 VCF file for the four datasets. To improve model performance, the effective population size
282 (N_e) of the first lineage of each pair was fixed based on π ($\pi=4N_e\mu$) (calculated in DnaSP 6,
283 based on all variant and invariant sites) (Excoffier & Foll, 2011). The other estimated
284 parameters were the N_e of the second lineage of the pair, the ancestral population size (N_{ANC}),
285 and the divergence time (T_{DIV}) for the scenario of strict divergence. In turn, for the scenario of
286 divergence with gene flow, two additional parameters were estimated: the migration rates
287 backward in time from population 1 to population 2 (MIG_1) and from population 2 to
288 population 1 (MIG_2).

289 For both coalescent models (divergence with and without gene flow), we assumed a
290 generation time of one year and a mutation rate (μ) of 2.24×10^{-8} , as estimated for a closely
291 related species (Thomaz et al., 2017). This mutation rate is appropriate for *Nematocharax*
292 because it was calculated from the regression formula for cellular organisms (Lynch, 2010)
293 based on the average genome size of Characidae ‘clade C’, where *Nematocharax* is
294 positioned (Thomaz et al., 2010). A total of 40 replicates were run for each dataset and
295 model, with 250,000 simulations per likelihood estimate, a stopping criterion of 0.001, and
296 10-40 expectation-conditional maximization (ECM). We obtained 95% confidence intervals
297 of parameters from 100 parametric bootstraps by simulating 100 SFS from the maximum
298 likelihood estimates and re-estimating parameters with 40 runs for each SFS. The best model
299 for each lineage pair was selected based on the AIC values calculated using the R script
300 ‘calculateAIC.sh’
301 (<http://github.com/speciationgenomics/scripts/blob/master/calculateAIC.sh>).

302

303 **Inferred drainage rearrangements from bathymetric and geomorphological data**

304

305 To test for a correspondence between genetic structure and the current configuration
306 of basins or historical drainage rearrangements due to headwater captures and coastal
307 paleodrainages, we applied GIS techniques to infer putative drainage rearrangements between
308 the NMA river basins. We reconstructed the putative paleodrainages that would have formed
309 during periods of low sea level using bathymetric and topographic data at 30 arc seconds
310 resolution obtained from the General Bathymetric Chart of the Oceans (GEBCO,
311 <http://www.gebco.net/>). These data were processed using the Hydrological tools in ArcGis10
312 following the methods described in Thomaz et al. (2015) (see also the reconstruction in
313 Thomaz & Knowles, 2018 for the entire Brazilian coast). Using the inferred connections
314 among currently isolated rivers implied by the coastal paleodrainage reconstruction, we
315 verified whether populations sampled in contemporary rivers within a paleodrainage are
316 genetically more similar to each other than populations from rivers located in different
317 paleodrainages.

318 We also inferred putative headwater captures in the Central region of the NMA
319 following the methodology described in Barreto et al. (2020), which uses the QGIS software
320 to analyze geological and geomorphological information that, according to de Oliveira
321 (2010), suggest the occurrence of this type of drainage rearrangement, particularly: (1)
322 elbows of capture (abrupt changes in drainage direction at approximately 90°; Bishop, 1995)
323 detected from the Continuous Cartographic Base of the Brazilian hydrography at 1:250,000
324 scale (DGC, 2017); (2) wind gaps (dry valleys that cross watershed divides and correspond to
325 ancient river beds; Ollier & Pain, 2000) identified from the SRTM 90 m Digital Elevation
326 Data (Jarvis et al., 2008); and (3) geological faults (areas of possible tectonic reactivation; de
327 Oliveira, 2010) obtained from the SD.24 Salvador sheet (DGC, 2016). These three data
328 sources were analyzed in QGIS 3.4.1 (QGIS Development Team, 2019) and, using the
329 inferred headwater captures, we evaluated whether there is a spatial correspondence between
330 the drainage rearrangements and the distribution of the *Nematocharax* clusters recovered by
331 the mtDNA and genomic data.

332

333 **RESULTS**

334

335 **Spatial and temporal inferences based on mtDNA**

336

337 The alignment of 295 COI sequences resulted in 46 haplotypes (93 variable sites)
338 distributed in nine mitochondrial lineages of *N. venustus* and one lineage of *N. varii*,
339 according to the BAPS analysis (Figures 2 and 3a). Based on the time-calibrated mtDNA
340 phylogeny (Figure 2), the earliest divergence between *N. varii* (lineage 10) and *N. venustus*
341 (lineages 1-9) date to the late Pliocene (2.88 Mya; 95% HPD = 3.67-2.16 Mya), while
342 divergences within *N. venustus* date to the Pleistocene. Using the BAPS assignment at the
343 tips of the mitochondrial time-calibrated tree, we found reciprocal monophyly for most
344 lineages, except mtDNA lineage 4 (see Figure 2) that was recovered as paraphyletic but with
345 low support values (<0.7). Genetic diversity varied across mitochondrial lineages (Table S5),
346 with the highest haplotype diversity being found in lineages 1 and 8 (13 and 12 haplotypes,
347 respectively), whereas some lineages were fixed for the same haplotype (i.e., lineages 3 and
348 10). In addition, significant negative Tajima's *D*-values and Fu's *F_s* were detected in five
349 lineages (Table S5).

350 Geographically, we found mtDNA lineages restricted to particular basins (lineage 1
351 from Contas; lineages 2 and 3 from Almada; lineages 4 and 9 from Cachoeira/Santana; and
352 lineages 6 and 7 from Pardo) and others shared among basins (lineage 5 from Cachoeira and
353 Una, and lineage 8 from Contas, Pardo, and Jequitinhonha; see Figure 1). Regarding the
354 watersheds with multiple mtDNA lineages, our results also show geographically structured
355 populations within basins (in the upstream versus downstream regions of the Contas,
356 Cachoeira, and Pardo river basins). Lineage 10 isolated in the Upper Contas River basin is
357 the only one that corresponds to the species *N. varii* (Figure 1).

358

359 **Genomic structure and diversification history**

360

361 The sNMF analysis of genomic data (Figure 3b) indicated three groups ($K = 3$) as the
362 best clustering for *N. venustus*. These groups encompass different mitochondrial lineages
363 with evidence of admixture among them. The first group (light gray) comprises mtDNA
364 lineages 2, 3, 4, and 5, corresponding to the small coastal basins of Almada,
365 Cachoeira/Santana, and Una. Lineage 5 is the only one in this group that occurs in more than
366 one river basin (i.e., Cachoeira and Una). The second group (dark gray) includes mtDNA
367 lineages 7 and 8, from the large basins of Contas, Pardo, and Jequitinhonha. In this case,
368 lineage 8 shows a wider distribution, occurring in these three basins. Lastly, the third group
369 (black) contains the mtDNA lineage 9, which is restricted to the Santana River, a small
370 tributary of the Cachoeira River basin (Figure 3b; also see map in Figure 1). Interestingly,

371 one sample collected in the Santana River (sample code 0684; Figures 3 and S1), although it
372 presented a higher ancestry coefficient for this group (black), differed from the other
373 individuals from that locality for presenting the mtDNA lineage 4 (which was detected in
374 another portion of the Cachoeira River basin). The remaining individuals for which we
375 obtained RADseq data correspond to mtDNA lineages 1 and 6, which exhibited the highest
376 levels of admixture among the three recovered genomic groups.

377 Regarding the evolutionary relationships from the MSC tree (Figure 3c), we observed
378 river basins characterized by reciprocally monophyletic groups (e.g. Almada) and river basins
379 where lineages have more than one origin (e.g. Contas in green and Cachoeira in orange),
380 some of them occurring in sympatry (see Figure 1). Both ML and Bayesian phylogenetic
381 trees using concatenated genomic data recovered the mtDNA lineages with high support
382 values, except for lineages 2/3 and 4/9 from Almada and Santana rivers, respectively, which
383 were grouped within mixed clusters (Figure S1).

384 Our divergence model tests showed which scenario best fits the data of each lineage
385 pair within *Nematocharax* (see Figure 3c and Table 1). Specifically, divergence without gene
386 flow (i.e., strict divergence) showed a better fit than divergence with gene flow for pair 1 (i-
387 ii; divergence between *N. varii* and *N. venustus*) and pair 4 (vii-viii; divergence between
388 small coastal basins – Almada, Cachoeira, and Una – and the Contas). In the first case (pair
389 1), we recovered much older divergence times between the two species of *Nematocharax*
390 than those estimated by mtDNA. On the other hand, pair 4 represents the most recent
391 divergence within *N. venustus*, during the Late Pleistocene (~17 kya). With respect to pair 2
392 (iii-iv; divergence between the lineage from the Cachoeira/Santana River basin and the
393 others) and pair 3 (v-vi; divergence between the lineage from the large river basins – Contas,
394 Pardo, and Jequitinhonha – and the remaining groups), divergence with gene flow was
395 inferred as the best fit model (Table 1). When analyzing the migration rates and direction of
396 movement across drainages (Table 1; Figure 3c), we observe that they were probably
397 asymmetric over time, occurring mainly from small coastal basins to the Santana River and
398 large river basins.

399

400 **Comparison between genetic structure and drainage rearrangements**

401

402 The reconstruction of coastal paleodrainages for the Central NMA shows that the past
403 and current configuration of rivers are largely congruent (see Figure 1; also see Thomaz &
404 Knowles, 2018). One exception is the Una and Pardo river basins, which were connected on

405 the exposed continental shelf during sea level retreats. Our paleodrainage reconstruction also
406 revealed an additional paleo-connection within the Cachoeira River basin, between the main
407 river and the Santana River, which are currently connected only by the estuary (Figure 1).

408 Our geomorphological analysis identified nine putative headwater captures between
409 drainages across the distribution of *Nematocharax* (Figures 1 and 4). Specifically, these
410 points represent past connections between: Contas and Almada (captures a and b), Almada
411 and Cachoeira (capture c), Contas and Cachoeira (captures d and e), Contas and Pardo
412 (capture f), Cachoeira and Pardo (capture g), Cachoeira and Una (capture h), and Pardo and
413 Jequitinhonha (capture i). This type of event may have occurred multiple times during the
414 geological history of these basins, allowing dispersal/isolation of fish lineages throughout the
415 area.

416 The comparison between the genetic structure found in *N. venustus* and the location of
417 putative drainage rearrangements shows that both mitochondrial and genomic data (see
418 Figure 3) do not reflect the reconstructed coastal paleo-connection between Una and Pardo
419 river basins (Figure 1) because the populations sampled within this paleodrainage do not
420 share a common ancestry. On the other hand, the presence of one sample in the Santana River
421 basin (sample code 0684) that has evidence of genomic admixture and belongs to the mtDNA
422 lineage 4 corroborates the more extensive coastal paleo-connection between the Santana and
423 Cachoeira rivers that allowed dispersal of freshwater fish across the continental shelf (Figures
424 1 and 3). Likewise, we observed the best fit of the ‘divergence with gene flow’ model for this
425 pair (pair 2; Table 1). Note that because of the match between current basin boundaries and
426 coastal paleodrainage boundaries (Figure 1) the effect of the remaining coastal
427 paleodrainages cannot be tested.

428 Among the nine inferred headwater captures (Figures 1 and 4), three of them are
429 supported by the geographic distribution of mtDNA lineages (specifically, headwater
430 captures labeled f, h, and i), whereas four putative past connections are suggested by the
431 genomic clusters; headwater captures c and h (Figure 1) would explain the composition of the
432 light gray cluster (Figure 3b), which includes the small coastal basins of Almada, Cachoeira,
433 and Una, and headwater captures f and i (Figure 1) help understand the geographic
434 distribution of the dark gray cluster (Figure 3b), including the secondary contact of lineages
435 (1-8) in the Contas River basin. Our RADseq data indicate that both the Contas and
436 Cachoeira river basins (green and orange, respectively) were colonized twice (see Figure 3c).

437

438 **DISCUSSION**

439

440 The geographic isolation of river basins within the NMA has no doubt been a major
441 factor in promoting differentiation, as evidenced by the clear spatial structuring of genetic
442 diversity in *Nematocharax*. However, our analyses suggest a dynamic history in which past
443 connections among these currently isolated basins have also shaped the geographic
444 structuring of genetic variation within *Nematocharax*. Our work then shows that paleo-
445 landscapes, as with terrestrial organisms, are an important factor in understanding the current
446 distribution of genetic structure in riverine fishes, especially considering the obvious
447 constraints imposed by a freshwater lifestyle. Additionally, as predicted by some models that
448 consider the river architecture (see Thomaz et al., 2016), we find evidence of genetic
449 differentiation within river basins, which illustrates the effect of the complex architecture of
450 rivers on the evolutionary dynamics of local populations.

451

452 **The role of drainage rearrangements in *Nematocharax* diversification**

453

454 Our results indicate a mixed history for the central basins of the NMA ecoregion, in
455 which long-term isolation among watersheds largely dictated the genetic structuring in
456 *Nematocharax*, but drainage rearrangements that allowed historical movement across
457 drainage divides probably also left a noticeable signature on patterns of genetic divergence. It
458 is known that other geomorphological processes can facilitate dispersal of organisms between
459 basins, such as divide inundation during flooding and swamps on low drainage divides that
460 form intermittent wet connections (Burrige et al., 2008). However, this may not be the case
461 in the NMA, because tectonic reactivation of ancient faults and erosive processes are known
462 to have caused several events of headwater capture along the eastern margin of the Brazilian
463 crystalline shield, where the watershed divides are generally formed by mountainous
464 landscapes (Ribeiro, 2006; Buckup, 2011). It is estimated that tectonic reactivations in this
465 region are as recent as <1.6 Mya (Saadi et al., 2002).

466

467 In this context, the first divergence within the genus (between *N. varii* and *N.*
468 *venustus*) took place in the Mio-Pliocene, a period during which tectonic events reactivated
469 old faults in the Espinhaço Range, where the Upper Contas River basin is located (Saadi,
470 1995). Given the geological and geomorphological processes related to the mountainous
471 relief in the Upper Contas River, the evolutionary history of *Nematocharax* is perhaps
472 marked by the complete isolation of *N. varii* in the highlands of the Chapada Diamantina

472 (Barreto, Nunes et al., 2016), which explain the best fit of the ‘divergence without gene flow’
473 model for pair 1.

474 Within *N. venustus*, we identified mtDNA lineages distributed across currently
475 isolated basins and divergent genomic lineages within a single basin (e.g. those associated
476 with the river basins in green and orange). These divergence histories probably took place in
477 the Pleistocene, although estimates based on COI sequences differed significantly from those
478 based on RADseq data. This is not unexpected given the methodological differences between
479 divergence time estimates of calibrated phylogenetic trees and coalescent-based models
480 (Edwards & Beerli, 2000; Carsten & Knowles, 2007). Regarding the Santana River, in the
481 Cachoeira River basin (in orange), we found two divergent lineages in both mitochondrial
482 (lineages 4 and 9) and genomic dataset, thus likely reflecting the effect of glacial cycles that
483 resulted in repeated sea level shifts and, consequently, repeated events of colonization
484 through coastal paleodrainages. Currently, the connection between the Cachoeira and Santana
485 rivers is possible only by the estuary, which represents an effective barrier to dispersal of
486 obligate freshwater fish from one river to another. This seems to be the case of
487 *Nematocharax*, given its little or no tolerance for saltwater (Wilzbach & Cummins, 2008).
488 Thus, sea level fluctuations during the Pleistocene may have allowed dispersal from the
489 Cachoeira to Santana River due to the expansion of this freshwater connection in periods of
490 sea regression, with subsequent isolation in periods of transgression. This hypothesis is
491 reinforced by the best fit of the ‘divergence with gene flow’ model (pair 2), in which the
492 migration rate was higher to the Santana River, in addition to the geomorphological evidence
493 of paleo-connection between the Cachoeira and Santana rivers on the continental shelf. We
494 also found one individual in the Santana River whose mtDNA is more related to individuals
495 from other portions of the Cachoeira River basin.

496 For the remaining river basins, the paleodrainage reconstruction reveals limited
497 connectivity between currently isolated rivers systems during sea level retreats because of the
498 relatively narrow continental shelf of the Central NMA, whereas the evidence of headwater
499 captures is widely distributed in the studied area. These results agree with the assumption that
500 the narrower and shallower northeastern Brazilian continental shelf would have imposed
501 conspicuous geographic isolation and eventually high levels of endemism in freshwater and
502 estuarine fish species (e.g. Baggio et al., 2017; Thomaz & Knowles, 2018; Argolo et al.,
503 2020). Therefore, putative dispersal routes via headwater captures are presented herein based
504 on evidence of elbows of capture (sudden shifts in the course of a river), wind gaps (dry
505 valleys once occupied by a river), and geological faults (areas possibly associated with

506 tectonic reactivations; see de Oliveira, 2010; Barreto et al., 2020). The signs of demographic
507 expansion for five mtDNA lineages also support that headwater capture events provided
508 opportunities for population expansion (Burrige et al., 2006; Waters et al., 2020).

509 By comparing the genetic structure recovered by mtDNA and the genomic loci, we
510 can assume that past connections allowed mitochondrial movement, and the paths of genomic
511 divergence were also redirected. For instance, individuals of *N. venustus* with morphological
512 and genetic differences were found at the point of sympatry between mtDNA lineages 1 and
513 8 (see sampling point '1*8' in the Contas River basin; Barreto et al., 2020). This locality is
514 close to the division between the Contas and Pardo river basins, where a putative headwater
515 capture was suggested (see capture f), which may have allowed the secondary contact and
516 hybridization between these lineages (Barreto et al., 2020), with strong support for a
517 population expansion in lineage 8. In fact, our divergence model test recovered 'divergence
518 with gene flow' for pair 3, which is in accordance with the hypothesis of connection between
519 these groups.

520

521 **Influence of past and current riverscape on genetic structuring**

522

523 Given that shared lineages are found among small coastal basins (i.e., Almada,
524 Cachoeira, and Una) as well as among large basins (i.e., Contas, Pardo, and Jequitinhonha), it
525 suggests that past connections along the Central NMA ecoregion fostered widespread
526 movement (i.e., they are not restricted geographically). If we consider that the elbow of
527 capture is close to the captor river (Bishop, 1995), our inferred headwater captures show that
528 most captor rivers belong to the small coastal basins (see captures a, b, c, d, and h), which
529 agrees with the direction of movement inferred for the lineage pairs. Moreover, the close
530 relationship recovered among basins is mirrored by faunal distribution patterns in other fish
531 species, including groups with different ecologies (e.g. Camelier & Zanata, 2014; Rodrigues
532 et al., 2016; de Sousa et al., 2021). This congruence in distribution patterns give insights
533 about the past configuration of the NMA rivers, suggesting that historical connections may
534 have structured communities more generally (i.e., the temporary connections are not species-
535 specific).

536 Despite support for nine putative headwater captures, correspondence between
537 geomorphological and genetic data was not observed for all putative headwater captures,
538 meaning that not all putative headwater captures appear to have facilitated movement. This
539 can be explained by a possible mismatch in timing between the occurrence of the river

540 capture event and the presence of fish. Dispersal may also simply not be likely depending on
541 the ephemerality of headwater capture events or species dispersal ability. In either case,
542 future investigations with other fish species will be important to test the generality of these
543 potential explanations. This is relevant because, although the drainage rearrangements
544 presented here may have similarly influenced the evolution of other co-distributed fish
545 species, whether temporary connections are available to fish may depend upon species-
546 specific ecologies (Tschá et al., 2017; Thomaz & Knowles, 2020; Waters et al., 2020).
547 Particularly in *Nematocharax*, some biological features such as restricted dispersal capacity
548 typical of small-sized characins (Lucas & Baras, 2001) and the potential influence of sexual
549 selection (Menezes et al., 2015; Barreto, Nunes, et al., 2016) may help explain the occurrence
550 of endemic groups and significant genetic differentiation among lineages in different river
551 basins, despite the evidence of temporary connections.

552 Although little is known about the *Nematocharax* biology, field and aquarium
553 observations indicate that territorial behavior can be observed especially in males (Barreto et
554 al., 2020), and the species probably occupies microenvironments within streams, completing
555 its life cycle in restricted geographic areas (Cetra et al., 2009). These features help understand
556 the reduced gene flow between populations, with local structuring and co-occurrence of
557 distinct lineages within river basins, as in the Cachoeira and Pardo. This structuring is
558 accentuated by the characteristics of the riverscape, such as the differential degree of
559 branching and basin slope at different portions of the river, with direct impacts on travel
560 distances and dispersal costs for fishes (Campbell Grant et al., 2007; Carvajal-Quintero et al.,
561 2019). Given that long-term population persistence is mainly dependent on connectivity,
562 investigating how riverscape heterogeneity influences spatial genetic structure (see Thomaz
563 et al., 2016) is essential to infer the evolutionary consequences of habitat loss and
564 fragmentation (Davis et al., 2018), factors that have continuously threatened the biodiversity
565 in basins along the Atlantic coast of Brazil (Menezes et al., 2007; Nogueira et al., 2010).
566 Moreover, elucidating the historical interconnectedness of these isolated basins becomes a
567 source of information for guiding conservation efforts, especially because the boundaries of
568 unique evolutionary units may not necessarily correspond to the current configuration of
569 basins.

570

571 CONCLUSIONS

572

573 Our study shows that a hidden genetic diversity in an endemic fish group has been
574 shaped by the isolated basins within the NMA ecoregion, as well as by some historical
575 temporary connections forged between them. However, in general, these river basins have
576 their own independent evolutionary histories, according to the geographic distribution of
577 *Nematocharax* lineages, with a few notable exceptions in which drainage rearrangements
578 structured divergence histories that are estimated here. These results contrast with genetic
579 studies of Neotropical fish from southern and southeastern Brazilian coastal basins (e.g.
580 Thomaz et al., 2015), reflecting the particular features of the NMA region, especially its
581 narrow continental shelf. As such, our findings demonstrate the importance of integrating
582 different data sources to generate hypotheses about when and where connections formed
583 between isolated river systems, and how they may have structured evolutionary divergence
584 and diversification of aquatic lineages.

585

586 **ACKNOWLEDGEMENTS**

587

588 We thank Angela Zanata (UFBA), Priscila Camelier (UFBA), and Daniel Carvalho (PUC
589 Minas) for providing some tissue samples used in this study, and the Knowles Lab for hosting
590 SSB at the University of Michigan, as well as providing computational resources. We also
591 thank the Rede de Plataformas Tecnológicas for the use of its Sequencing Facility in
592 FIOCRUZ-Bahia, the Core Facility for Scientific Research – University of São Paulo
593 (CEFAP-USP/GENIAL) for the use of its Illumina NextSeq sequencer, and the National
594 Laboratory for Scientific Computing (LNCC/MCTI, Brazil) for providing HPC resources of
595 the SDumont supercomputer, which have contributed to the research results reported within
596 this paper. This study was financially supported by CAPES (Finance Code 001,
597 23038.000776/2017-54, PDSE 88881.186858/2018-01, and 88882.453923/2019-01),
598 FAPESB (RED0045/2014 and JCB0026/2016), and CNPq (465767/2014-1). HB-F
599 acknowledges the CNPq Research Productivity fellowship (307037/2018-5). SBB thanks
600 CAPES for the postdoctoral fellowship (grant 88887.474651/2020-00).

601

602 **DATA AVAILABILITY STATEMENT**

603

604 COI sequences: GenBank accession numbers MN011168-MN011188 and MN011203-
605 MN011363.

606

607 **CONFLICT OF INTEREST STATEMENT**

608

609 The authors have no conflicts of interest to declare.

610

611 **REFERENCES**

612

613 Abell, R., Thieme, M. L., Revenga, C., Bryer, M., Kottelat, M., Bogutskaya, N., ... Petry, P.
614 (2008). Freshwater ecoregions of the world: a new map of biogeographic units for

615 freshwater biodiversity conservation. *BioScience*, 58(5), 403–414. DOI: 10.1641/B580507

616 Albert, J. S., & Reis, R. E. (2011). Historical biogeography of Neotropical freshwater fishes.

617 Berkeley, CA: University of California Press.

618 Albert, J. S., Craig, J. M., Tagliacollo, V. A., & Petry, P. (2018). Upland and lowland fishes:

619 a test of the river capture hypothesis. Chapter 19. In: Mountains, climate and biodiversity.

620 (Eds: C. Hoorn, A. Perrigo & A. Antonelli). Wiley-Blackwell, New York.

621 Albert, J. S., Petry, P., & Reis, R. E. (2011). Major biogeographic and phylogenetic patterns.

622 Chapter 2. In: Historical biogeography of Neotropical freshwater fishes. (Eds: J. S. Albert

623 & R. E. Reis). University of California Press, Berkeley.

624 Argolo, L. A., López-Fernández, H., Batalha-Filho, H., & Affonso, P. R. A. M. (2020).

625 Unraveling the systematics and evolution of the ‘*Geophagus*’ *brasiliensis* (Cichliformes:

626 Cichlidae) species complex. *Molecular Phylogenetics and Evolution*, 150, 106855. DOI:

627 10.1016/j.ympev.2020.106855

628 Baggio, R. A., Stoiev, S. B., Spach, H. L., & Boeger, W.A. (2017). Opportunity and taxon

629 pulse: the central influence of coastal geomorphology on genetic diversification and

630 endemism of strict estuarine species. *Journal of Biogeography*, 44(7), 1626–1639. DOI:

631 10.1111/jbi.12934

632 Barreto, S. B., Cioffi, M. B., Medrado, A. S., Silva, A. T., Affonso, P. R. A. M., & Diniz, D.

633 (2016). Allopatric chromosomal variation in *Nematocharax venustus* Weitzman, Menezes

634 & Britski, 1986 (Actinopterygii: Characiformes) based on mapping of repetitive

635 sequences. *Neotropical Ichthyology*, 14(2), e150141. DOI: 10.1590/1982-0224-20150141

636 Barreto, S. B., Knowles, L. L., Affonso, P. R. A. M., & Batalha-Filho, H. (2020). Riverscape

637 properties contribute to the origin and structure of a hybrid zone in a Neotropical

638 freshwater fish. *Journal of Evolutionary Biology*, 33(11), 1530–1542. DOI:

639 10.1111/jeb.13689

- 640 Barreto, S. B., Nunes, L. A., Silva, A. T., Jucá-Chagas, R., Diniz, D., Sampaio, I., ... Affonso,
641 P. R. A. M. (2016). Is *Nematocharax* (Actinopterygii, Characiformes) a monotypic fish
642 genus?. *Genome*, 59(10), 851–865. DOI: 10.1139/gen-2015-0166
- 643 Barreto, S. B., Silva, A. T., Batalha-Filho, H., Affonso, P. R. A. M., & Zanata, A. M. (2018).
644 Integrative approach reveals a new species of *Nematocharax* (Teleostei: Characidae).
645 *Journal of Fish Biology*, 93(6), 1151–1162. DOI: 10.1111/jfb.13834
- 646 Bishop, P. (1995). Drainage rearrangement by river capture, beheading and diversion.
647 *Progress in Physical Geography*, 19(4), 449–473. DOI: 10.1177/030913339501900402
- 648 Buckup, P. A. (2011). The Eastern Brazilian Shield. Chapter 12. In: Historical biogeography
649 of Neotropical freshwater fishes. (Eds: J. S. Albert & R. E. Reis). University of California
650 Press, Berkeley.
- 651 Burridge, C. P., Craw, D., & Waters, J. M. (2006). River capture, range expansion, and
652 cladogenesis: the genetic signature of freshwater vicariance. *Evolution*, 60(5), 1038–1049.
653 DOI: 10.1111/j.0014-3820.2006.tb01181.x
- 654 Burridge, C. P., Craw, D., Jack, D. C., King, T. M., & Waters, J. M. (2008). Does fish
655 ecology predict dispersal across a river drainage divide?. *Evolution*, 62(6), 1484–1499.
656 DOI: 10.1111/j.1558-5646.2008.00377.x
- 657 Camelier, P., & Zanata, A. M. (2014). Biogeography of freshwater fishes from the
658 Northeastern Mata Atlântica freshwater ecoregion: distribution, endemism, and area
659 relationships. *Neotropical Ichthyology*, 12(4), 683–698. DOI: 10.1590/1982-0224-
660 20130228
- 661 Camelier, P., Menezes, N. A., Costa-Silva, G. J., & Oliveira, C. (2018). Molecular and
662 morphological data of the freshwater fish *Glandulocauda melanopleura* (Characiformes:
663 Characidae) provide evidences of river captures and local differentiation in the Brazilian
664 Atlantic Forest. *PLOS One*, 13(3), e0194247. DOI: 10.1371/journal.pone.0194247
- 665 Campbell Grant, E. H., Lowe, W. H., & Fagan, W. F. (2007). Living in the branches:
666 population dynamics and ecological processes in dendritic networks. *Ecology Letters*,
667 10(2), 165–175. DOI: 10.1111/j.1461-0248.2006.01007.x
- 668 Carstens, B. C., & Knowles, L. L. (2007). Shifting distributions and speciation: species
669 divergence during rapid climate change. *Molecular Ecology*, 16(3), 619–627. DOI:
670 10.1111/j.1365-294X.2006.03167.x
- 671 Carvajal-Quintero, J., Villalobos, F., Oberdorff, T., Grenouillet, G., Brosse, S., Hugueny, B.,
672 ... Tedesco, P. A. (2019). Drainage network position and historical connectivity explain

673 global patterns in freshwater fishes' range size. *Proceedings of the National Academy of*
674 *Sciences*, 116(27), 13434–13439. DOI: 10.1073/pnas.1902484116

675 Cetra, M., Ferreira, F. C., & Carmassi, A. L. (2009). Caracterização das assembléias de
676 peixes de riachos de cabeceira no período chuvoso na bacia do rio Cachoeira (SE da
677 Bahia, NE do Brasil). *Biota Neotropica*, 9(2), 107–115. DOI: 10.1590/S1676-
678 06032009000200010

679 Chifman, J., & Kubatko, L. (2014). Quartet inference from SNP data under the coalescent
680 model. *Bioinformatics*, 30(23), 3317–3324. DOI: 10.1093/bioinformatics/btu530

681 Clark, P. U., Dyke, A. S., Shakun, J. D., Carlson, A. E., Clark, J., Wohlfarth, B., ... McCabe,
682 A. M. (2009). The Last Glacial Maximum. *Science*, 325(5941), 710–714. DOI:
683 10.1126/science.1172873

684 Corander, J., & Marttinen, P. (2006). Bayesian identification of admixture events using
685 multilocus molecular markers. *Molecular Ecology*, 15(10), 2833–2843. DOI:
686 10.1111/j.1365-294X.2006.02994.x

687 Darriba, D., Taboada, G. L., Doallo, R., & Posada, D. (2012). jModelTest 2: more models,
688 new heuristics and parallel computing. *Nature Methods*, 9(8), 772–772. DOI:
689 10.1038/nmeth.2109

690 Davis, C. D., Epps, C. W., Flitcroft, R. L., & Banks, M. A. (2018). Refining and defining
691 riverscape genetics: how rivers influence population genetic structure. *Wiley*
692 *Interdisciplinary Reviews: Water*, 5(2), e1269. DOI: 10.1002/wat2.1269

693 de Oliveira, D. (2010). Capturas fluviais como evidências da evolução do relevo: uma revisão
694 bibliográfica. *Revista do Departamento de Geografia*, 20, 37–50. DOI:
695 10.7154/RDG.2010.0020.0003

696 de Sousa, J. L. P., Bitencourt, J. A., Sampaio, I., Schneider, H., & Affonso, P. R. A. M.
697 (2021). “More than meets the eye”: phylogeographic inferences and remarkable cryptic
698 diversity and in endemic catfish *Parotocinclus* (Loricariidae: Hypoptopomatinae) from
699 neglected and impacted basins in South America. *Conservation Genetics*, 22, 411–425.
700 DOI: 10.1007/s10592-021-01336-3

701 Del Fabbro, C., Scalabrin, S., Morgante, M., & Giorgi, F. M. (2013). An extensive evaluation
702 of read trimming effects on Illumina NGS data analysis. *PLOS One*, 8(12), e85024. DOI:
703 10.1371/journal.pone.0085024

704 Dias, M. S., Oberdorff, T., Hugué, B., Leprieux, F., Jézéquel, C., Cornu, ... Tedesco, P. A.
705 (2014). Global imprint of historical connectivity on freshwater fish biodiversity. *Ecology*
706 *Letters*, 17(9), 1130–1140. DOI: 10.1111/ele.12319

707 Diretoria de Geociências (IBGE/DGC) (2016). Falhas Geológicas da Folha SD.24 –
708 Salvador. Retrieved from http://dados.gov.br/dataset/cren_geologiafalhasd24
709 Diretoria de Geociências (IBGE/DGC) (2017). BC250 - Base cartográfica contínua do Brasil
710 - 1:250 000. Retrieved from
711 http://geofitp.ibge.gov.br/cartas_e_mapas/bases_cartograficas_continuas/bc250/versao2017
712 Drummond, A. J., Suchard, M. A., Xie, D., & Rambaut, A. (2012). Bayesian phylogenetics
713 with BEAUti and the BEAST 1.7. *Molecular Biology and Evolution*, 29(8), 1969–1973.
714 DOI: 10.1093/molbev/mss075
715 Eaton, D. A. R. (2014). PyRAD: assembly of de novo RADseq loci for phylogenetic
716 analyses. *Bioinformatics*, 30(13), 1844–1849. DOI: 10.1093/bioinformatics/btu121
717 Edwards, S. V., & Beerli, P. (2000). Perspective: gene divergence, population divergence,
718 and the variance in coalescence time in phylogeographic studies. *Evolution*, 54(6), 1839–
719 1854. DOI: 10.1111/j.0014-3820.2000.tb01231.x
720 Excoffier, L., & Foll, M. (2011). Fastsimcoal: A continuous-time coalescent simulator of
721 genomic diversity under arbitrarily complex evolutionary scenarios. *Bioinformatics*, 27(9),
722 1332–1334. DOI: 10.1093/bioinformatics/btr124
723 Excoffier, L., Dupanloup, I., Huerta-Sánchez, E., Sousa, V. C., & Foll, M. (2013). Robust
724 demographic inference from genomic and SNP data. *PLOS Genetics*, 9(10), e1003905.
725 DOI: 10.1371/journal.pgen.1003905
726 Frichot, E., Mathieu, F., Trouillon, T., Bouchard, G., & François, O. (2014). Fast and
727 efficient estimation of individual ancestry coefficients. *Genetics*, 196(4), 973–983. DOI:
728 10.1534/genetics.113.160572
729 Fu, Y. X. (1997). Statistical tests of neutrality of mutations against population growth,
730 hitchhiking and background selection. *Genetics*, 147(2), 915–925.
731 Hales, J., & Petry, P. (2015). Northeastern Mata Atlantica ecoregion. Retrieved from
732 <http://www.feow.org/ecoregions/details/328>
733 Hughes, J. M., Schmidt, D. J., & Finn, D. S. (2009). Genes in streams: using DNA to
734 understand the movement of freshwater fauna and their riverine habitat. *BioScience*, 59(7),
735 573–583. DOI: 10.1525/bio.2009.59.7.8
736 Jarvis, A., Reuter, H. I., Nelson, A., & Guevara, E. (2008). Hole-filled seamless SRTM data
737 V4. International Centre for Tropical Agriculture (CIAT). Retrieved from
738 <http://srtm.csi.cgiar.org>

739 Knapp, I. S. S., Puritz, J., Bird, C., Whitney, J., Sudek, M., Forsman, Z., & Toonen R. (2016).
740 ezRAD - an accessible next-generation RAD sequencing protocol suitable for non-model
741 organisms_v3.2. Retrieved from <http://doi.org/10.17504/protocols.io.e9pbh5n>

742 Lima, S. M., Berbel-Filho, W. M., Araújo, T. F., Lazzarotto, H., Tatarenkov, A., & Avise, J.
743 C. (2017). Headwater capture evidenced by paleo-rivers reconstruction and population
744 genetic structure of the armored catfish (*Pareiorhaphis garbei*) in the Serra do Mar
745 mountains of southeastern Brazil. *Frontiers in Genetics*, 8, 199. DOI:
746 10.3389/fgene.2017.00199

747 Lima, S. M., Berbel-Filho, W. M., Vilasboa, A., Lazoski, C., de Assis Volpi, T., Lazzarotto,
748 H., ... Solé-Cava, A. M. (2021). Rio de Janeiro and other palaeodrainages evidenced by the
749 genetic structure of an Atlantic Forest catfish. *Journal of Biogeography*, 48(6), 1475–
750 1488. DOI: 10.1111/jbi.14091

751 Lucas, M., & Baras, E. (2001). Migration of freshwater fishes. Oxford, UK: Blackwell
752 Science Ltd.

753 Lynch, M. (2010). Evolution of the mutation rate. *Trends in Genetics*, 26(8): 345–352. DOI:
754 10.1016/j.tig.2010.05.003

755 Martins, L. R., & Coutinho, P. N. (1981). The Brazilian continental margin. *Earth-Science*
756 *Reviews*, 17(1-2), 87–107. DOI: 10.1016/0012-8252(81)90007-6

757 Menezes, N. A., & Lima, F. C. T. (2008). *Nematocharax venustus* Weitzman, Menezes &
758 Britski, 1986. In: Livro Vermelho da Fauna Brasileira Ameaçada de Extinção (Eds: A. B.
759 M. Machado, G. M. Drummond & A. P. Paglia). MMA, Brasília.

760 Menezes, N. A., Weitzman, S. H., Oyakawa, O. T., Lima, F. C. T. D., Correa e Castro, R. M.,
761 & Weitzman, M. J. (2007). Peixes de água doce da Mata Atlântica: lista preliminar das
762 espécies e comentários sobre conservação de peixes de água doce neotropicais. São Paulo,
763 SP: Museu de Zoologia da Universidade de São Paulo.

764 Menezes, N. A., Zanata, A. M., & Camelier, P. (2015). *Nematocharax costai* Bragança,
765 Barbosa & Mattos a junior synonym of *Nematocharax venustus* Weitzman, Menezes &
766 Britski (Teleostei: Characiformes: Characidae). *Zootaxa*, 3920(3), 453–462. DOI:
767 10.11646/zootaxa.3920.3.4

768 Miller, M. A., Pfeiffer, W., & Schwartz, T. (2010). Creating the CIPRES Science Gateway
769 for inference of large phylogenetic trees. In: Proceedings of the Gateway Computing
770 Environments Workshop. GCE, New Orleans.

771 Nogueira, C., Buckup, P. A., Menezes, N. A., Oyakawa, O. T., Kasecker, T. P., Neto, M. B.
772 R., & da Silva, J. M. C. (2010). Restricted-range fishes and the conservation of Brazilian
773 freshwaters. *PLOS One*, 5(6), e11390. DOI: 10.1371/journal.pone.0011390

774 Oliveira, C., Avelino, G. S., Abe, K. T., Mariguela, T. C., Benine, R. C., Ortí, G., ... Castro,
775 R. M. C. (2011). Phylogenetic relationships within the speciose family Characidae
776 (Teleostei: Ostariophysii: Characiformes) based on multilocus analysis and extensive
777 ingroup sampling. *BMC Evolutionary Biology*, 11, 275. DOI: 10.1186/1471-2148-11-275

778 Ollier, C., & Pain, C. (2000). The origin of mountains. London, UK: Routledge.

779 QGIS Development Team (2019). QGIS Geographic Information System, Open Source
780 Geospatial Foundation. Retrieved from <http://qgis.osgeo.org>

781 Rambaut, A., Drummond, A. J., Xie, D., Baele, G., & Suchard, M. A. (2018). Posterior
782 summarization in Bayesian phylogenetics using Tracer 1.7. *Systematic Biology*, 67(5),
783 901–904. DOI: 10.1093/sysbio/syy032

784 Rannala, B., Edwards, S. V., Leaché, A., & Yang, Z. (2020). The Multispecies Coalescent
785 Model and Species Tree Inference. Chapter 3.3. In: *Phylogenetics in the Genomic Era*.
786 (Eds: C. Scornavacca, F. Delsuc, & N. Galtier), No commercial publisher, Authors open
787 access book. Retrieved from <https://hal.inria.fr/PGE>

788 Ribeiro, A. C. (2006). Tectonic history and the biogeography of the freshwater fishes from
789 the coastal drainages of eastern Brazil: an example of faunal evolution associated with a
790 divergent continental margin. *Neotropical Ichthyology*, 4(2), 225–246. DOI:
791 10.1590/S1679-62252006000200009

792 Rodrigues, A. D. S., Brandão, J. H. S. G., Bitencourt, J. A., Jucá-Chagas, R., Sampaio, I.,
793 Schneider, H., & Affonso, P. R. A. M. (2016). Molecular identification and traceability of
794 illegal trading in *Lignobrycon myersi* (Teleostei: Characiformes), a threatened Brazilian
795 fish species, using DNA barcode. *The Scientific World Journal*, 2016, 9382613. DOI:
796 10.1155/2016/9382613

797 Ronquist, F., Teslenko, M., Van Der Mark, P., Ayres, D. L., Darling, A., Höhna, S., ...
798 Huelsenbeck, J. P. (2012). MrBayes 3.2: efficient Bayesian phylogenetic inference and
799 model choice across a large model space. *Systematic Biology*, 61(3), 539–542. DOI:
800 10.1093/sysbio/sys029

801 Rozas, J., Ferrer-Mata, A., Sánchez-DelBarrio, J. C., Guirao-Rico, S., Librado, P., Ramos-
802 Onsins, S. E., & Sánchez-Gracia, A. (2017). DnaSP 6: DNA sequence polymorphism
803 analysis of large data sets. *Molecular Biology and Evolution*, 34(12), 3299–3302. DOI:
804 10.1093/molbev/msx248

805 Saadi, A. (1995). A geomorfologia da Serra do Espinhaço em Minas Gerais e de suas
806 margens. *Geonomos*, 3(1), 41–63. DOI: 10.18285/geonomos.v3i1.215

807 Saadi, A., Machette, M. N., Haller, K. M., Dart, R. L., Bradley, L., & Souza, A. M. P. D.
808 (2002). Map and database of Quaternary faults and lineaments in Brazil. U.S. Geological
809 Survey Open-File Report 02-230. Version 1.0. Retrieved from
810 <http://pubs.usgs.gov/of/2002/ofr-02-230/>

811 Schwarzer, J., Swartz, E. R., Vreven, E., Snoeks, J., Cotterill, F. P. D., Misof, B., &
812 Schliewen, U. K. (2012). Repeated trans-watershed hybridization among haplochromine
813 cichlids (Cichlidae) was triggered by Neogene landscape evolution. *Proceedings of the*
814 *Royal Society B: Biological Sciences*, 279(1746), 4389–4398. DOI:
815 10.1098/rspb.2012.1667

816 Shelley, J. J., Swearer, S. E., Dempster, T., Adams, M., Le Feuvre, M. C., Hammer, M. P., &
817 Unmack, P. J. (2020). Plio-Pleistocene sea-level changes drive speciation of freshwater
818 fishes in north-western Australia. *Journal of Biogeography*, 47(8), 1727–1738. DOI:
819 10.1111/jbi.13856

820 Souza, M. S., Thomaz, A. T., & Fagundes, N. J. (2020). River capture or ancestral
821 polymorphism: an empirical genetic test in a freshwater fish using approximate Bayesian
822 computation. *Biological Journal of the Linnean Society*, 131(3), 575–584. DOI:
823 10.1093/biolinnean/blaa140

824 Stamatakis, A. (2014). RAxML version 8: a tool for phylogenetic analysis and post-analysis
825 of large phylogenies. *Bioinformatics*, 30(9), 1312–1313. DOI:
826 10.1093/bioinformatics/btu033

827 Swofford, D. L. (2003). PAUP*: phylogenetic analysis using parsimony and other methods,
828 version 4.0 b10. Sunderland, MA: Sinauer Associates.

829 Tajima, F. (1989). Statistical method for testing the neutral mutation hypothesis by DNA
830 polymorphism. *Genetics*, 123(3), 585–595.

831 Thomaz, A. T., & Knowles, L. L. (2018). Flowing into the unknown: inferred paleodrainages
832 for studying the ichthyofauna of Brazilian coastal rivers. *Neotropical Ichthyology*, 16(3),
833 e180019. DOI: 10.1590/1982-0224-20180019

834 Thomaz, A. T., & Knowles, L. L. (2020). Common barriers, but temporal dissonance:
835 Genomic tests suggest ecological and paleo-landscape sieves structure a coastal riverine
836 fish community. *Molecular Ecology*, 29(4), 783–796. DOI: 10.1111/mec.15357

- 837 Thomaz, A. T., Christie, M. R., & Knowles, L. L. (2016). The architecture of river networks
838 can drive the evolutionary dynamics of aquatic populations. *Evolution*, 70(3), 731–739.
839 DOI: 10.1111/evo.12883
- 840 Thomaz, A. T., Malabarba, L. R., & Bonatto, S. L. (2010). The phylogenetic placement of
841 *Hollandichthys* Eigenmann 1909 (Teleostei: Characidae) and related genera. *Molecular*
842 *Phylogenetics and Evolution*, 57(3), 1347–1352. DOI: 10.1016/j.ympev.2010.10.006
- 843 Thomaz, A. T., Malabarba, L. R., & Knowles, L. L. (2017). Genomic signatures of
844 paleodrainages in a freshwater fish along the southeastern coast of Brazil: genetic structure
845 reflects past riverine properties. *Heredity*, 119(4), 287–294. DOI: 10.1038/hdy.2017.46
- 846 Thomaz, A. T., Malabarba, L. R., Bonatto, S. L., & Knowles, L. L. (2015). Testing the effect
847 of palaeodrainages versus habitat stability on genetic divergence in riverine systems: study
848 of a Neotropical fish of the Brazilian coastal Atlantic Forest. *Journal of Biogeography*,
849 42(12), 2389–2401. DOI: 10.1111/jbi.12597
- 850 Thompson, J. D., Higgins, D. G., & Gibson, T. J. (1994). CLUSTAL W: improving the
851 sensitivity of progressive multiple sequence alignment through sequence weighting,
852 position-specific gap penalties and weight matrix choice. *Nucleic Acids Research*, 22(22),
853 4673–4680. DOI: 10.1093/nar/22.22.4673
- 854 Toonen, R. J., Puritz, J. B., Forsman, Z. H., Whitney, J. L., Fernandez-Silva, I., Andrews, K.
855 R., & Bird, C. E. (2013). ezRAD: a simplified method for genomic genotyping in non-
856 model organisms. *PeerJ*, 1, e203. DOI: 10.7717/peerj.203
- 857 Tschá, M. K., Baggio, R. A., Marteleto, F. M., Abilhoa, V., Bachmann, L., & Boeger, W. A.
858 (2017). Sea-level variations have influenced the demographic history of estuarine and
859 freshwater fishes of the coastal plain of Paraná, Brazil. *Journal of Fish Biology*, 90(3),
860 968–979. DOI: 10.1111/jfb.13211
- 861 Ward, R. D., Zemlak, T. S., Innes, B. H., Last, P. R., & Hebert, P. D. (2005). DNA barcoding
862 Australia's fish species. *Philosophical Transactions of the Royal Society B: Biological*
863 *Sciences*, 360(1462), 1847–1857. DOI: 10.1098/rstb.2005.1716
- 864 Waters, J. M., Burrige, C. P., & Craw, D. (2020). River capture and freshwater biological
865 evolution: a review of galaxiid fish vicariance. *Diversity*, 12(6), 216. DOI:
866 10.3390/d12060216.
- 867 Weitzman, S. H., Menezes, N. A., & Weitzman, M. J. (1988). Phylogenetic biogeography of
868 the Glandulocaudini (Teleostei: Characiformes, Characidae) with comments on the
869 distributions of other freshwater fishes in eastern and southeastern Brazil. In: Proceedings

870 of Workshop on Neotropical Distribution Patterns. (Eds: P. E. Vanzolini & W. R. Heyer).
871 Academia Brasileira de Ciências, Rio de Janeiro.

872 Wilzbach, M. A., & Cummins, K. W. (2008). Rivers and streams: Physical setting and
873 adapted biota. In: Encyclopedia of Ecology. (Eds: S. E. Jørgensen & B. D. Fath). Elsevier,
874 Oxford.

875 Winemiller, K. O., & Willis, S. C. (2011). The Vaupes Arch and Casiquiare Canal: Barriers
876 and Passages. Chapter 14. In: Historical biogeography of Neotropical freshwater fishes.
877 (Eds: J. S. Albert & R. E. Reis). University of California Press, Berkeley.

Author Manuscript

878 **FIGURE CAPTIONS**

879

880 **Figure 1.** Map of the Central region of the Northeastern Mata Atlantica (NMA) ecoregion
881 showing the collection sites of *Nematocharax* in the Contas, Almada, Cachoeira, Una, Pardo,
882 and Jequitinhonha river basins, which are color coded to demarcate their boundaries; small
883 coastal basins with no record of *Nematocharax* are shown in gray. The distribution of
884 different mitochondrial lineages (see Figures 2 and 3) is shown as numbers in black boxes;
885 note that an asterisk between numbers indicates collection sites with two mitochondrial
886 lineages (i.e., sympatry). Nine putative headwater captures inferred from geomorphological
887 data (which are detailed in Figure 4) are shown in red letters (a-i), and the reconstructed
888 coastal paleodrainages on the continental shelf during the period of largest drop in sea level
889 (LGM; up to 130 m) are shown by the dashed dark blue lines.

890

891 **Figure 2.** Time-calibrated Bayesian tree reconstructed by BEAST using COI sequences, with
892 lineages of *Nematocharax* color coded according to their basins (see map in Figure 1 for
893 details). Tips were collapsed into the 10 mitochondrial lineages according to the BAPS
894 assignment, with sample sizes (n) shown for each lineage. Numbers and bars on the nodes
895 show the estimated age and 95% highest probability density (HPD) intervals of the node age,
896 respectively.

897

898 **Figure 3.** Genetic structure within *N. venustus* based on (a) a Bayesian Analysis of
899 Population Structure (BAPS) using COI sequences ($n = 274$), with dashed lines separating
900 the nine mtDNA clusters (in which individuals are colored according to the river basins
901 where they were collected; Figure 1); b) K -genetic clusters ($n = 20$) inferred from the
902 genomic RADseq data with sNMF (light gray, dark gray, and black represent the three groups
903 recovered by the ancestry coefficients and which are separated by dashed lines; dashed lines
904 also show the correspondence between the genomic and mtDNA clusters. Some individuals
905 (those that correspond to mtDNA lineages 1 and 6) were not assigned to any specific
906 genomic cluster due to high levels of mixture (samples not delimited by dashed lines); c)
907 evolutionary relationships among individuals ($n = 20$) recovered by SVDquartets under the
908 multispecies coalescent (MSC) model using genomic data; the groups used in separate
909 fastsimcoal2 analyses for divergence model tests are marked at the nodes (i.e., the roman

910 numerals i through viii). In the same way as BAPS (a), the tips of the tree were colored
911 according to the river basins where the specimens were collected (see Figure 1).

912 *Sample collected in the Santana River with higher ancestry coefficient for the black group
913 but with mtDNA lineage 4

914 **Individuals from Jequitinhonha were poorly sequenced and therefore were not included in
915 the genomic analyses

916

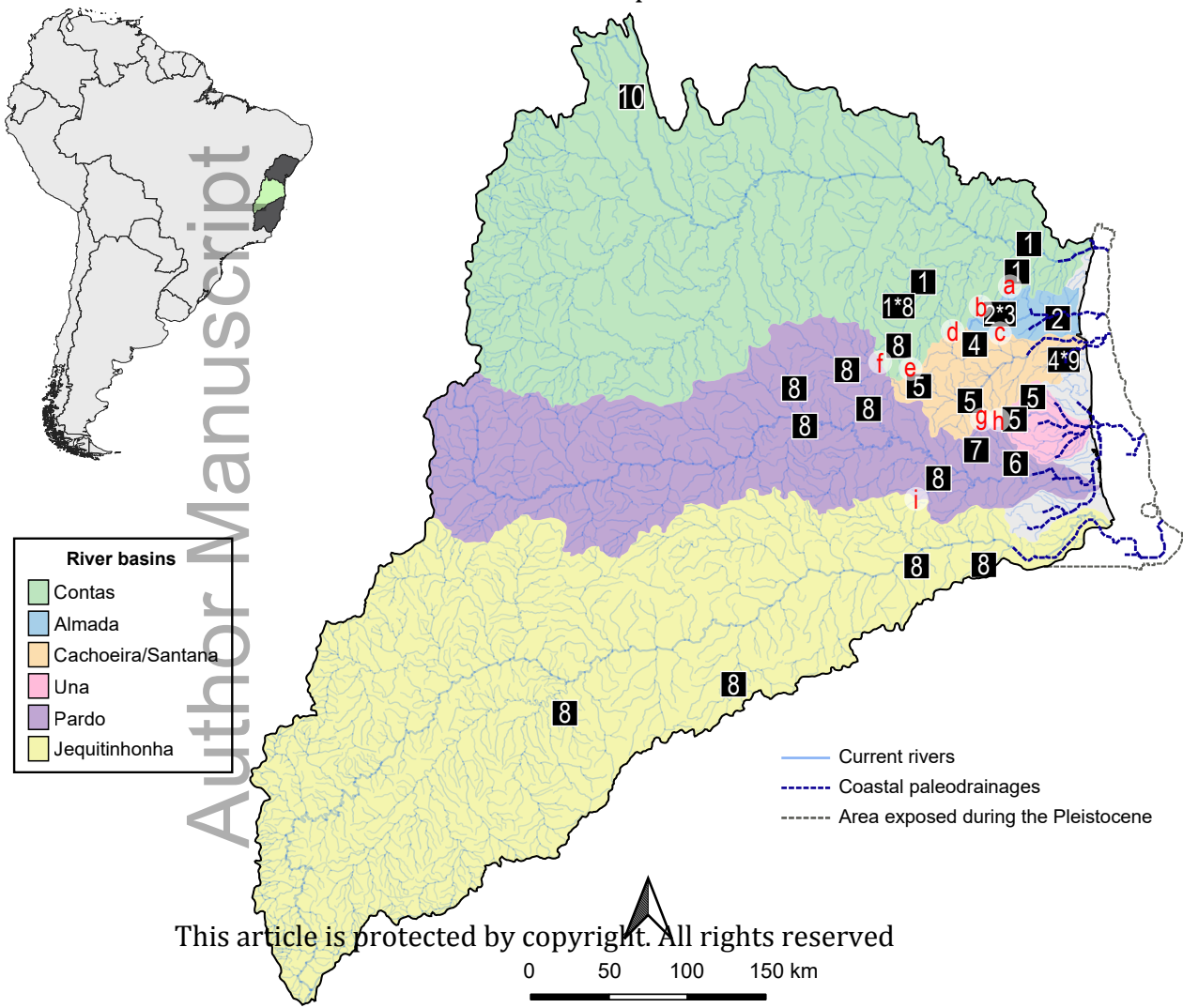
917 **Figure 4.** Putative headwater captures in the Central portion of the Northeastern Mata
918 Atlantica (NMA) ecoregion inferred from geomorphological data (i.e., a-i) and which are also
919 marked in Figure 1 (red letters) for an overview of the entire NMA. In these maps, current
920 rivers are in blue and red lines define the current watershed divides. The black and white
921 lines mark the location of geological faults (i.e., tectonic reactivation areas), and low to high
922 elevation is shown in dark to light shading, respectively. Wind gaps (i.e., dry valleys that
923 cross watershed divides) are highlighted in yellow, showing how currently isolated river
924 basins were connected in the past.

Author Manuscript

Table 1. Fastsimcoal2 results for the two tested divergence models (strict divergence and divergence with gene flow) for each lineage pair of *Nematocharax* (pairs i-ii, iii-iv, v-vi, and vii-viii; see Figure 3c) including the point estimate and 95% confidence interval in parentheses for each parameter. Specifically, the effective size of the first population of the pair (N_1 , fixed value calculated in DnaSP 6 based on all variant and invariant sites), effective size of the second population of the pair (N_2), ancestral population size (N_{ANC}), divergence time (T_{DIV}), and migration rates backward in time from population 1 to population 2 (MIG_1) and from population 2 to population 1 (MIG_2) are reported. Also shown are the number of loci used to calculate the site frequency spectrum (SFS) of each pair, for which the most likely divergence model, according to the lowest Akaike Information Criterion (AIC) value, is highlighted in bold.

Lineage pair	Loci	Model	N_1 (fixed)	N_2	N_{ANC}	T_{DIV} (in generations)	MIG_1	MIG_2	AIC
Pair 1 (i-ii)	1,686	Strict divergence	3,414	10,312,417 (5,597,783–6,142,663)	9,682,982 (9,551,329–10,417,296)	19,860,219 (6,052,532–6,955,249)	na	na	8514.61
		Divergence with gene flow		5,676,862 (276,563–3,911,478)	4,608,404 (4,421,946–10,322,358)	13,081,732 (236,948–8,783,860)	1.48e-4 (3.40e-5–1.93e-4)	1.37e-4 (7.43e-4–0.10)	8659.22
Pair 2 (iii-iv)	873	Strict divergence	4,103	10,407,940 (3,900,968–4,716,178)	10,144,034 (8,702,434–9,234,337)	5,587,253 (1,601,304–2,061,663)	na	na	5760.33
		Divergence with gene flow		557,737 (139,608–5,014,358)	10,315,367 (7,443,758–8,414,510)	9,092 (6,709–1,353,093)	0.17 (0.07–0.21)	5.58e-3 (2.04e-4–4.79)	3871.94
Pair 3 (v-vi)	3,820	Strict divergence	16,781	7,442,637 (3,233,745–3,608,029)	10,131,818 (8,037,969–8,374,713)	3,445,100 (1,359,940–1,596,286)	na	na	40322.87
		Divergence		8,839,016 (169,147–	10,294,640	161,609 (12,643–	0.63 (0.16–0.64)	0.03 (3.41e-4–	21202.70

		with gene flow	4,650,537)	(7,701,936–8,318,601)	1,382,357)		3.63)		
Pair 4 (vii-viii)	8,841	Strict divergence	15,517	15,702 (14,791–17,040)	36,782 (34,846–38,255)	16,931 (15,975–17,956)	na	na	33650.76



This article is protected by copyright. All rights reserved

0 50 100 150 km

